JNeurosci
THE JOURNAL OF NEUROSCIENCE

Research Articles | Behavioral/Cognitive

Disentangling the Spatiotemporal Neural Dynamics of Conflict Detection and Resolution between Lexical and Sublexical Processes in Oral Word Reading: An Intracranial SEEG Study

https://doi.org/10.1523/JNEUROSCI.1183-26.2026

Received: 13 July 2026
Revised: 8 October 2026
Accepted: 6 November 2026

Copyright © 2026 the authors

This Early Release article has been peer reviewed and accepted, but has not been through the composition and copyediting processes.The final version may differ slightly in style or formatting and will contain links to any extended data.

Alerts: Sign up at www.jneurosci.org/alerts to receive customized email alerts when the fully formatted version of this article is published.

Title

Disentangling the Spatiotemporal Neural Dynamics of Conflict Detection and Resolution between Lexical and Sublexical Processes in Oral Word Reading: An Intracranial SEEG Study

Abbreviated title

Conflict Detection and Resolution Dynamics

Authors

Chunyu Zhao[1]†, Yi Liu[2]†, Jiahong Zeng[1], Xiangqi Luo[1], Zhiyun Dai,[1] Xuliang Zhang[1], Yidong Jiang[1], Yuxin Liu[1], Zuyun Li[1], Gaofeng Shi[3], Yumei Zhang[4], Weijin Sun[5], Yuguang Guan[5*], Zaizhu Han[1*]

Affiliations

[1] National Key Laboratory of Cognitive Neuroscience and Learning, Beijing Normal University, Beijing 100875, China.

[2] Beijing Institute of Otolaryngology, Otolaryngology-Head and Neck Surgery, Beijing Tongren Hospital, Capital Medical University, Beijing 100005, China.

[3] College of International Education and Exchange, Tianjin Normal University, Tianjin 300387, China.

[4] Department of Rehabilitation Medicine, Beijing Tiantan Hospital, Capital Medical University, Beijing 100070, China.

[5] Department of Neurosurgery, Sanbo Brain Hospital, Capital Medical University, Beijing 100093, China.

[*]Address correspondence to: Zaizhu Han, zzhhan@bnu.edu.cn, No.19, Xinjiekouwai Street, Haidian District, Beijing, 100875, China and Yuguang Guan, guanyg2020@ccmu.edu.cn, Building 1, Yard 36, Dongba Middle Road, Chaoyang District, Beijing, 100018, China.

JNeurosci Accepted Manuscript

†These authors contributed equally to this work.

Conflict of interests

The authors declare no competing financial interests.

Acknowledgments

This work was supported by the Major Project of National Social Science Foundation of China (24&ZD252) and the National Natural Science Foundation of China (32671399, 32271091, and 82301300). We extend our thanks to the BNU-Han Lab members for their helpful suggestions and all research participants for their cooperation.

JNeurosci Accepted Manuscript

Abstract

Object recognition relies on correspondence between whole objects and their subcomponents. When this correspondence is disrupted, accurate recognition requires detecting conflicts and inhibiting misleading subcomponent information, yet the neural basis underlying these processes remain unclear. Written language, with sublexical components that may conflict with whole words, provides an ideal testbed. Using stereo-electroencephalography (SEEG) recorded from 39 participants (both sexes) during Chinese character reading, we revealed a functional dissociation between neural systems supporting conflict detection and inhibitory control. Conflict detection was associated with β band activity in the fusiform gyrus and widespread θ and α band effects across temporal and parietal regions. Inhibitory control was associated with α and β band activity in the inferior frontal and precentral gyri. Granger causality analysis showed increased β band connectivity from conflict-processing to inhibitory-control regions under conflict conditions. These findings demonstrate that disruptions of whole-sublexical correspondence engage dissociable neural systems for conflict detection and inhibitory control, implemented through frequency- and region-specific neural oscillations and coordinated via increased information transfer from posterior to frontal regions.

Significance Statement

Reading often requires resolving conflicts between competing linguistic representations, yet the neural mechanisms that detect such conflicts and resolve them remain poorly understood. Using stereo-electroencephalography with millimeter-scale spatial and millisecond-scale temporal resolution, we dissociated sublexical conflict detection from inhibitory control during Chinese character reading. We show that these processes are supported by distinct low-frequency oscillatory networks and are linked through directed functional interactions. These findings move beyond traditional accounts of sublexical effects by identifying their underlying cognitive components and neural dynamics, providing a mechanistic

JNeurosci Accepted Manuscript

framework for understanding how cognitive control supports fluent word recognition.

Key words

Word reading, Conflict detection, Inhibitory control, Neural oscillations, SEEG

JNeurosci Accepted Manuscript

INTRODUCTION

Throughout evolution, organisms have acquired the capacity for rapid and accurate object recognition, which depends not only on holistic information but also on object subcomponents. This is because subcomponents in natural object is typically congruent with the whole object, facilitating recognition by enhancing both accuracy and processing speed (e.g., leopard spots predict a leopard). However, some of man-made objects have mismatched information between whole and its components. This is especially evident in written words, where long-term sound and meaning changes have disrupted the original part-whole correspondence established by regular construction principles. For instance, the pronunciation /*jɑːt*/ of the English word “yacht” cannot be derived from the pronunciations of its components “ya” or “ch” (Borgwaldt et al., 2005; Libben et al., 2003).

Such a mismatch creates competition between whole-character and sublexical phonological information; successful reading therefore requires detecting and resolving this conflict. Evidence for these processes comes mainly from previously reported regularity and consistency effects (Coltheart et al., 2001; Kang & Saito, 2025; Lee, 2008; Martensen et al., 2000; Yum et al., 2014; C. Zhao et al., 2024). The regularity effect reflects whether a phonetic radical (a component that may provide a cue to pronunciation) matches the whole character in pronunciation. For example, “喂” is regular because it and its phonetic radical “畏” are both pronounced /*wei4*/; when they mismatch, the character is irregular. In contrast, the consistency effect reflects pronunciation consistency within a phonetic family: a family is consistent when most characters sharing a phonetic radical have the same pronunciation, but inconsistent when they have multiple pronunciations. For example, characters containing “皇” (e.g., “蝗,” “惶,” and “煌”) are all pronounced /*huang2*/, and thus form a consistent family; whereas characters containing “青” (e.g., “清” /*qing1*/, “猜” /*cai1*/, and “精” /*jing1*/) have different pronunciations and thus form an inconsistent family. Behaviorally, irregular and inconsistent words typically elicit longer response times (RTs) than regular and consistent words (Dang et al., 2019; Lee et al., 2005; X. Zhou &

JNeurosci Accepted Manuscript

Marslen-Wilson, 1999), which is thought to reflect extra processing to resolve competing phonological information, including inhibitory control over conflicting or unreliable sublexical information.

Neuroimaging studies have further identified neural mechanisms that detect whole-sublexical conflicts and resolve them by inhibiting sublexical representations. Event-related potential (ERP) studies show that whole-sublexical correspondence influences neural activity from the N170 to the P200 and N400, suggesting that different forms of sublexical information are processed at distinct stages during word recognition (Hsu et al., 2011; Yum et al., 2014; Yum & Law, 2019; L. Zhou et al., 2014; L. Zhou & Perfetti, 2021). Complementary functional magnetic resonance imaging (fMRI) and lesion studies indicate that these effects are supported by a distributed fronto-temporo-parietal network (Borghesani et al., 2020; Regev et al., 2024; Yang et al., 2011; J. Zhao et al., 2012). More broadly, conflict detection and inhibitory control are associated with low-frequency neural oscillations, particularly in the θ, α, and β bands, and distributed cortical regions (Cavanagh & Frank, 2014; Hwang et al., 2014; Miller & Cohen, 2001; Pscherer et al., 2023). Together, these findings suggest that whole-sublexical conflict detection and resolution rely on distributed neural networks operating across multiple temporal and spectral scales.

While previous studies have documented the behavioral and neural correlates of conflict detection and resolution through various sublexical effects, several issues remain. First, conflict detection and resolution have typically been examined together rather than dissociated, because contrasts based on sublexical conflict levels inevitably confound detection with the additional inhibitory demands of resolution. Second, their neural networks have not been characterized with sufficient spatiotemporal resolution, as fMRI and ERP each have limitations in spatial and temporal precision. Third, the interaction between these networks remains largely unexplored, despite the fact that conflict detection and resolution operate as coordinated processes during spoken word reading (Schaum et al., 2021; Thiebaut De Schotten & Forkel, 2022).

JNeurosci Accepted Manuscript

To address these issues, we recruited 39 participants undergoing clinically indicated stereo-electroencephalography (SEEG), which offers millimeter-scale spatial and millisecond-scale temporal resolution, and asked them to perform a Chinese character oral reading task. Stimuli were categorized into different conditions (see Methods for details) based on the relationship between phonetic radicals and whole-character pronunciations. Using linear mixed-effects model (LMM), we dissociated the neural dynamics of conflict detection and inhibitory control across frequency bands and anatomical regions. Furthermore, Granger causality analysis (GCA) revealed connectivity from conflict-related to inhibition-related regions.

MATERIALS AND METHODS

Participants

Thirty-nine epilepsy patients (11 females; mean age = 24.36, *SD* = 8.03, range: 12~43) were recruited, and all underwent SEEG implantation for clinical treatment. They were native Mandarin speakers with an average of 12.15 years of education (*SD* = 3.24, range: 5~17), ensuring their ability to complete the Chinese character reading tasks in this study. Written informed consent was obtained from all participants, and the study was approved by the Institutional Review Board of the last corresponding author's institution. These participants were drawn from a publicly available dataset (C. Zhao et al., 2024), and detailed demographic and clinical information are summarized in ***Table S1***.

Experimental materials and procedure

The reading materials consisted of commonly used Chinese compound characters, each containing a phonetic radical that provides cues to pronunciation. Stimuli were characterized along two distinct dimensions of sublexical phonological effects: regularity and consistency. Regularity was defined as the correspondence between the pronunciation of a phonetic radical and that of the whole character (see ***Figure 1A***). For example, the regular character "喂" (/*wei4*/, which denotes syllable and tone) contains the phonetic radical "畏" (/*wei4*/), which

JNeurosci Accepted Manuscript

reliably indicates its pronunciation. Irregular characters such as “婢” (/*bi4*/) contain phonetic radicals, “卑” (/*bei1*/), whose pronunciation differs from the whole character. Consistency was defined based on whether a phonetic radical consistently predicts the pronunciations of different characters within the same phonetic family. For example, characters containing the radical “皇” (e.g., 蝗, 惶, 煌) are all pronounced /*huang2*/, indicating a consistent phonetic family. In contrast, characters containing the radical “青” (e.g., 清 /*qing1*/, 猜 /*cai1*/, and 精 /*jing1*/) have different pronunciations despite sharing the same radical, indicating an inconsistent phonetic family.

Based on the two dimensions, the characters were categorized into three conditions: regular-consistent (RC), regular-inconsistent (RiC), and irregular-inconsistent (iRiC). Notably, irregular-consistent characters do not exist in Chinese. A total of 120 characters were included in the current study, with 40 characters in each condition. Word frequency of these characters was balanced across conditions. Stimuli were presented using Psychtoolbox (Brainard, 1997). As shown in ***Figure 1B***, each trial began with a fixation cross displayed for a variable duration (0~1000 ms), followed by a 2000 ms blank screen. A Chinese character then appeared for 1000 ms, during which participants were required to read the character aloud as accurately and quickly as possible. The task comprised six blocks, each containing 20 characters pseudo-randomly drawn from the 120 Chinese characters. Each block was balanced across the three conditions (RC, RiC, and iRiC), and the stimulus order was randomized within blocks to minimize potential order effects.

Behavioral data: acquisition, preprocessing, and analysis

Participants’ oral reading responses were automatically recorded using Psychtoolbox. The recordings of each character were imported into Adobe Audition (2022) for manual annotation of RT and accuracy (ACC). To examine whether the sublexical consistency and regularity effects persist when accounting for random effects of participants, LMMs for RT and generalized linear mixed-effects models (GLMMs) for ACC were fitted in MATLAB (R2022a, MathWorks

JNeurosci Accepted Manuscript

Inc.) using the *fitlme* and *fitglme* functions from the Statistics and Machine Learning Toolbox, respectively. Both models included experimental condition (comparing RC vs. RiC and RiC vs. iRiC) as a fixed effect and random intercept for participants. The model formulas were:

$$RT \sim Condition + (1 \mid Participant) \quad (1)$$

$$ACC \sim Condition + (1 \mid Participant) \quad (2)$$

where *RT* denotes response time, *ACC* is pronunciation accuracy, and *Condition* is the experimental manipulation. The term *(1 | Participant)* accounts for individual variability by including random intercepts across participants. For ACC, a binomial distribution with a logit link function was used, and the Laplace approximation was applied to ensure convergence and stable parameter estimation.

SEEG data acquisition

Across the 39 participants, 401 electrodes comprising 5,703 contacts were implanted (mean = 14.22 per electrode, *SD* = 2.78, range = 8~18). Contacts located at electrode ends or within seizure zones were excluded, resulting in 2524 contacts included in the recordings. The SEEG signals were recorded using BrainAmp amplifiers (Brain Products) at a sampling rate of 5000 Hz, and were referenced online to a scalp contact at the vertex.

SEEG data preprocessing

Contact Localization

To identify contacts' anatomical labels, each participant's pre-implantation structural MRI was coregistered with their post-implantation CT using the FieldTrip toolbox (Oostenveld et al., 2011). The resulting contact coordinates were then normalized to the standard Montreal Neurological Institute (MNI) template to allow for group-level analysis.

Signal preprocessing

Using EEGLAB (Delorme & Makeig, 2004), the signals were first downsampled to 1000 Hz and re-referenced using the average reference. Subsequently, data were bandpass filtered between 0.05 and 200 Hz and notch

JNeurosci Accepted Manuscript

filtered at 50, 100, and 150 Hz. The continuous recordings were divided into 3000 ms epochs (−1000 to 2000 ms relative to stimulus onset). Epochs were rejected if they contained incorrect trials or outlier RTs (>3 *SD*s).

Time-frequency transformation

Time-frequency representations (TFRs) of the SEEG signals were computed by convolving the preprocessed data with complex Morlet wavelets (0.5~40 Hz in 0.5 Hz steps; 7-cycle width) within a time window of −800 to 800 ms relative to stimulus onset (in 4 ms steps), using the FieldTrip. Spectral power was then averaged across trials for each contact. Contacts with impedance greater than 15 kΩ or TFR values exceeding 3 *SD*s were considered outliers and excluded from further analyses.

Identification of responsive contacts

To identify responsive contacts, TFRs were computed as a time-frequency transformation, except that spectral power was computed for individual trials without averaging. A non-parametric cluster-based permutation *t*-test (point-level $p < 0.05$, 1000 randomizations) was performed to compare power between the active (0 to 800 ms) and baseline (−800 to 0 ms) windows for each contact (Maris & Oostenveld, 2007). Contacts showing significant positive or negative clusters (cluster-level $p < 0.05$) were deemed responsive and assigned anatomical labels based on the Anatomical Automatic Labeling (AAL) template; nonresponsive contacts were excluded from further analyses.

SEEG data processing and statistical analysis

General sublexical effects

Motivated by prior links between low-frequency oscillations (θ, α, β) and conflict processing and inhibitory control during sublexical processing (Cavanagh & Frank, 2014; Hwang et al., 2014; Pscherer et al., 2023; Schaum et al., 2021), we examined general sublexical effects at the group level by computing trial-averaged TFRs for each responsive contact under RC, RiC, and iRiC, normalized as percentage changes from a −300 to −100 ms pre-stimulus baseline, yielding

JNeurosci Accepted Manuscript

ERSPs. Condition-wise differences in ERSP were assessed using a cluster-based permutation *t*-test (point-level two-tailed $p < 0.05$, 1000 randomizations), within the 0~800 ms post-stimulus window across all responsive contacts. Specifically, general consistency (RC vs. RiC) and regularity (RiC vs. iRiC) effects were identified. Effects were considered significant if cluster-level corrected *p*-values were below 0.05.

RT-controlled sublexical effects

General sublexical effects, obtained from condition contrasts, provide information about overall sublexical processing but do not disentangle the neural contributions of distinct subprocesses. To examine oscillatory signature of RT-controlled sublexical effects, trial-level TFRs were first extracted for each contact within θ (4~7 Hz), α (8~12 Hz), and β (13~30 Hz) bands. For each participant and AAL region, band-specific ERSPs were then obtained by averaging TFRs across all contacts and normalizing them as percentage changes from baseline (−300 to −100 ms). To enhance the generalizability and reliability of the results, subsequent analyses were limited to brain regions with ≥ 20 responsive contacts from ≥ 10 participants (all 12 brain regions included in the subsequent analyses are listed in ***Table 1***). To isolate sublexical effects from variability in RT, while also controlling for subject-level random effects, trial-level LMM was fitted with condition and RT as fixed effects and random intercepts for participants. These model formulas were:

$$\theta \sim Condition + RT + (1 \mid Participant) \quad (3)$$

$$\alpha \sim Condition + RT + (1 \mid Participant) \quad (4)$$

$$\beta \sim Condition + RT + (1 \mid Participant) \quad (5)$$

where θ, α, and β denote the band-specific ERSP, *Condition* reflects the experimental manipulation (RC vs. RiC or RiC vs. iRiC), and *RT* captures trial-wise variation in response time. The term *(1 | Participant)* accounts for individual variability by including random intercepts across participants. Finally, a cluster-based permutation test was conducted to identify significant clusters (point-level two-tailed $p < 0.05$, 1000 randomizations).

JNeurosci Accepted Manuscript

RT-associated sublexical effects

We next investigated the oscillatory signature of RT-associated sublexical effects. Because our analyses included only trials with correct pronunciation responses, conflicting trials reflected successful resolution of the whole–sublexical conflict. Thus, variation in RT among correct trials captures the processing demands of successful conflict resolution, including the inhibitory control of competing sublexical information. We therefore included trial-level RT in the LMMs to examine the neural correlates of this process. LMMs were fitted with RT as the dependent variable, θ, α, and β band ERSPs as fixed effects under RiC and iRiC conditions, and participant as a random intercept:

$$RT \sim \theta + \alpha + \beta + (1 \mid Participant), Condition \in \{RiC, iRiC\} \quad (6)$$

where *RT* denotes trial-level response time, and *θ, α,* and *β* represent band-specific ERSP amplitudes. The term *(1 | Participant)* accounts for individual variability by including random intercepts across participants. Similarly, significant clusters were identified using the cluster-based permutation test (point-level two-tailed $p < 0.05$, 1000 randomizations).

To test whether the observed ERSP-RT associations were specific to RT-associated sublexical effects rather than general RT-related effects, two control analyses were performed. First, we applied the same LMMs in the RC condition to assess whether similar ERSP-RT associations could be observed:

$$RT \sim \theta + \alpha + \beta + (1 \mid Participant), Condition \in \{RC\} \quad (7)$$

Second, we fitted an additional model across all three conditions (RC, RiC, iRiC), including experimental condition as a random factor:

$$RT \sim \theta + \alpha + \beta + (1 \mid Participant) + (1 \mid Condition) \quad (8)$$

In this extended model, *(1 | Participant)* and *(1 | Condition)* account for individual and condition-related variability as random intercepts.

Finally, to directly test whether the ERSP-RT associations differed across experimental conditions, we additionally fitted LMMs including θ, α, and β ERSPs, condition, and their interaction terms in the model:

$$RT \sim \theta * Condition + \alpha * Condition + \beta * Condition + (1 \mid Participant) \quad (9)$$

JNeurosci Accepted Manuscript

In this extended model, *Condition* was treated as a three-level factor (RC, RiC, and iRiC), with interaction effects tested for RiC vs. RC and iRiC vs. RC.

Directed connectivity between sublexical processing regions

Building on our previous analyses that identified brain regions with distinct sublexical effects, we next examined the modulatory relationships among them. To this end, we applied GCA (Granger, 1969; Stokes & Purdon, 2017) to assess effective connectivity between regions showing RT-controlled vs. RT-associated effects. To prevent overfitting due to excessive parameter estimation in the following multivariate autoregressive (MVAR) modeling (Barnett & Seth, 2014), preprocessed SEEG data were further down-sampled to 100 Hz and processed with linear detrending, first-order differencing, and mean voltage removal to enhance stationarity. Due to the lack of prior research on feedback frequency bands, the analysis was not divided into predefined bands (θ, α, or β), but instead evaluated directed connectivity across a continuous frequency range.

MVAR models were then fitted to the processed SEEG signals from all regional contacts within each experimental condition, defined as:

$$X_{(t)} = \sum_{k=1}^{p} A_k X_{(t-k)} + \varepsilon_{(t)} \quad (10)$$

where $X_{(t)}$ is the multivariate signal vector at time t across all channels; p is the model order, set to 20 (200 ms temporal lag), chosen to capture low-frequency directional connectivity within a 400 ms sliding window (−400 to 800 ms relative to stimulus onset, in 10 ms steps); A_k is the $m \times m$ autoregressive coefficient matrix at lag k; and $\varepsilon_{(t)}$ denotes the error vector at time t. Subsequently, the estimated coefficient matrices were transformed into the frequency domain via the Fourier transformation. At each frequency f, the frequency response function $H(f)$ was computed as:

$$H(f) = \left(I - \sum_{k=1}^{p} A_k e^{-i2\pi f k / f_s}\right)^{-1} \quad (11)$$

where f denotes the frequency, A_k is the MVAR coefficient matrix at lag k, and f_s is the sampling rate, I is the identity matrix. Based on this, the cross-spectral density matrix $S(f)$ was obtained:

$$S(f) = H(f) \cdot \Sigma_e \cdot H(f)^H \quad (12)$$

JNeurosci Accepted Manuscript

where Σ_e denotes the error covariance matrix, and $H(f)^H$ is the conjugate transpose of $H(f)$. Finally, Granger causality values (GCVs) were derived using the Granger-Geweke estimator (Geweke, 1982).

$$F_{i\to j}(f) = ln\left(\frac{S_{ii}(f)}{S_{ii}(f)-\left(\Sigma_{jj}-\left(\Sigma_{ij}^2/\Sigma_{ii}\right)\right)\cdot|H_{ij}(f)|^2}\right) \quad (13)$$

Where $F_{i\to j}(f)$ denotes the spectral granger causality from channel i to channel j at frequency f; $S_{ii}(f)$ is the auto-spectral density of channel i at frequency f; Σ is the noise covariance matrix estimated from the MVAR model; $H_{ij}(f)$ is the (i,j) element of the transfer function matrix $H(f)$.

For the pathways from PoCG, MTG, ITG, FG, and PCun to IFG-tri and PrCG, there were 10 potential connections. Three pathways (FG→PrCG, PCun→IFG-tri, and PCun→PrCG) were excluded due to an insufficient number of contact pairs (<10) for reliable statistical inference. The final connectivity analysis focused on 7 pathways: PoCG→IFG-tri, PoCG→PrCG, MTG→IFG-tri, MTG→PrCG, ITG→IFG-tri, ITG→PrCG, and FG→IFG-tri. Given the heterogeneous electrode coverage across patients, GCA were conducted pairwise for each pathway, rather than using a multivariate GCA including all regions simultaneously. Finally, to evaluate the statistical significance of stimulus-evoked GCVs, post-stimulus data (0~800 ms) were compared to a pre-stimulus baseline (−400 to −200 ms) across contacts for each experimental condition. For the statistical significance of stimulus-evoked connectivity, post-stimulus GCVs (0~800 ms) were compared to baseline (−400~−200 ms) across contact pairs for each experimental condition. For condition comparisons, GCVs from the post-stimulus window were directly contrasted across conditions. In both analyses, cluster-based permutation tests (point-level two-tailed $p < 0.05$, 1000 randomizations) were used to control for multiple comparisons.

Data availability

The SEEG data from a publicly available dataset (https://osf.io/mkz2r/). The analysis scripts in the current study are openly available at https://osf.io/yp6zu/.

JNeurosci Accepted Manuscript

RESULTS

Behavioral performance

In the behavioral analysis, RTs were fitted using an LMM (R^2 = 0.233), and ACC was fitted using a GLMM (R^2 < 0.001). A likelihood ratio test showed no significant effect of condition on accuracy (χ^2 = 3.586, p = 0.167). In contrast, there was a significant main effect of condition on RT (χ^2 = 12.987, p = 0.002). Post-hoc tests revealed that RTs were significantly shorter in the RC condition (M = 702 ms, SD = 153 ms) than in the RiC condition (M = 715 ms, SD = 162 ms) (β = 0.013, F = 6.753, p = 0.009), indicating a significant consistency effect. However, RTs in the RiC condition were not significantly shorter than those in the iRiC condition (M = 719 ms, SD = 162 ms) (β = 0.005, F = 0.763, p = 0.382). These results showed a significant consistency effect on RT, whereas neither consistency nor regularity significantly affected accuracy.

Whole-brain time-frequency patterns of general sublexical effects

Whole-brain averaged time-frequency analyses revealed that differences between conditions were primarily observed in the α and β bands. As shown in ***Figure 2D***, in the α band, activity was enhanced in the RiC condition relative to RC, but reduced in iRiC relative to RiC. Conversely, in the β band, RiC elicited weaker activity than RC over a broad temporal window (approximately 100~700 ms post-stimulus), whereas iRiC evoked stronger activity than RiC within an earlier time window (approximately 200 ms post-stimulus). These findings indicate that sublexical processing is associated with differential α and β band activity, with α band effects showing opposite modulation patterns and β band effects differing in both direction and temporal dynamics. Notably, these whole-brain averaged effects do not necessarily reflect the temporal or spatial patterns within individual brain regions. The anatomical specificity and regional temporal characteristics of these effects were further examined in subsequent analyses.

JNeurosci Accepted Manuscript

Regional oscillatory correlates of RT-controlled sublexical effects

The LMM model fit results (R^2) for the RT-controlled consistency effect and regularity effect are presented in ***Figure S1*** and ***Figure S2***, respectively. A significant consistency effect was observed in the fusiform gyrus (FG) (***Figure 3A***), where β band ERSP differed between the RiC and RC conditions approximately from 596 to 684 ms post-stimulus (cluster-level corrected p = 0.048). In contrast, RT-controlled regularity effects were observed in multiple brain regions, including the postcentral gyrus (PoCG), middle temporal gyrus (MTG), inferior temporal gyrus (ITG), FG, and precuneus (PCun) (***Figure 3B***). Specifically, θ band activity differed significantly between conditions in the PoCG (approximately 440~652 ms, cluster-level corrected p = 0.036), while α activity in the MTG (approximately 276~800 ms, cluster-level corrected p = 0.002), ITG (approximately 80~224 ms, cluster-level corrected p = 0.042), FG (approximately 396~672 ms, cluster-level corrected p = 0.016), and PCun (approximately 524~732 ms, cluster-level corrected p = 0.024) showed significant RT-controlled sublexical effects of regularity. These results indicate that consistency and regularity contrasts were associated with distinct neural oscillatory patterns, with the consistency effect relatively focal and late, and the regularity effect involving multiple regions with earlier and more sustained activity.

Regional oscillatory correlates of RT-associated sublexical effects

The LMM model fit results (R^2) for the RT-associated sublexical effects in the RiC and iRiC conditions are presented in ***Figure S3*** and ***Figure S4***, respectively. In the RiC condition (***Figure 4A***), the significant associations between ERSP and RT were observed in the inferior frontal gyrus, triangular part (IFG-tri), precentral gyrus (PrCG), and inferior temporal gyrus (ITG). Specifically, β band activity in the IFG-tri (approximately 468~600 ms) was negatively associated with RT (cluster-level corrected p = 0.038). In the PrCG, α activity (approximately 564~800 ms) showed a positive association (cluster-level corrected p = 0.032), whereas β activity (approximately 592~752 ms) exhibited a negative association (cluster-level corrected p = 0.030). In the ITG, β band activity (approximately 656~800 ms) also

JNeurosci Accepted Manuscript

demonstrated a significant negative association (cluster-level corrected $p = 0.030$). For the iRiC condition (***Figure 4B***), significant effects were observed in the IFG-tri and calcarine sulcus (CS). Specifically, α band activity in the IFG-tri (approximately 192~368 ms) was positively associated with RT (cluster-level corrected $p = 0.034$), while β band activity in the CS (approximately 712~800 ms) showed a significant negative association (cluster-level corrected $p = 0.048$).

To determine whether the ERSP-RT associations identified above were specific to conflicting conditions rather than reflecting general RT-related neural activity, we conducted two control analyses. First, the same LMM for the RC condition revealed that, except for a marginal β band effect in the superior temporal gyrus (STG; approximately 700~800 ms, cluster-level corrected $p = 0.050$) (***Figure S5A***), no other significant effects were observed. To further validate this, ERSPs were averaged within the significant clusters identified in the RiC and iRiC conditions and re-entered into the model. The results showed that, except for β activity in the CS, which also showed a significant association in the RC condition ($\beta = 0.017$, $t = 2.057$, $p = 0.040$), none of the ERSP features predictive of RT under RiC and iRiC were associated with RT in the RC condition (βs < 0.012, ts < 1.269, ps > 0.205). Second, we fitted an additional model across all the three conditions, including condition as a random intercept. It revealed a β band effect in the PrCG (approximately 632~744 ms; cluster-level corrected $p = 0.040$) and CS (approximately 696~800 ms; cluster-level corrected $p = 0.040$) (***Figure S5B***). We then repeated the analysis using averaged ERSPs from the significant clusters identified in the RiC and iRiC conditions. The results showed that β activity in the IFG-tri, PrCG, and ITG, which was previously predictive of RT under RiC (βs > 0.009, ts > 2.167, ps < 0.031), as well as β activity in the CS, which was previously predictive of RT under iRiC ($\beta = 0.017$, $t = 2.912$, $p = 0.004$), significantly associated with RT. In contrast, none of the other significant clusters identified under RiC or iRiC showed significant associations with RT (βs < 0.005, ts < 1.197, ps > 0.231). These results indicate that, after accounting for nonspecific RT-related effects, α band activity in the IFG-tri and PrCG remained selectively associated with RT under conflict conditions.

J Neurosci Accepted Manuscript

Finally, we directly tested whether the ERSP-T relationships differed between conditions. In an exploratory analysis, we tested the interactions between ERSP and condition separately for θ, α, and β band activity for each brain region. No significant interaction was observed for either RiC versus RC (cluster-level corrected *p*s > 0.063) or iRiC vs. RC (cluster-level corrected *p*s > 0.081) across any frequency band or brain region. We therefore conducted a ROI-based follow-up analysis for the regions identified in the RT-associated analysis, averaging ERSPs within the previously identified significant temporal clusters and entering them into the LMMs with ERSP × condition interactions. Significant α-ERSP × condition interactions were observed in the IFG-tri for iRiC vs. RC (β = 0.018, t = 2.425, p = 0.015) and in the PrCG for RiC vs. RC (β = 0.020, t = 2.066, p = 0.039). No significant interaction was found in the other regions shown in ***Figure 4*** for either RiC vs. RC (βs < 0.025, ts < 1.653, ps > 0.098) or iRiC vs. RC (βs < 0.012, ts < 0.810, ps > 0.418). These findings further indicate that the relationships between α-ERSP and RT in the IFG-tri and PrCG were condition-specific, differing between conflict and non-conflict conditions.

Directed connectivity between sublexical processing regions

The GCA results between brain regions showing RT-controlled and RT-associated sublexical effects are shown in ***Figure 5***. Four pathways showed significant directed connectivity: two in the RC condition (PoCG→IFG-tri and ITG→IFG-tri), two in the RiC condition (PoCG→IFG-tri and ITG→IFG-tri), and three in the iRiC condition (FG→IFG-tri, ITG→IFG-tri, and ITG→PrCG). In the RC condition, 12~27 Hz connectivity from the PoCG to the IFG-tri was reduced relative to baseline throughout the post-stimulus period (cluster-level corrected p = 0.002), and 4~8 Hz connectivity from the ITG to the IFG-tri was reduced approximately from 50 to 250 ms (cluster-level corrected p = 0.044). In the RiC condition, connectivity from the PoCG to IFG-tri increased in the β band (15~24 Hz) during two clusters (approximately 50~250 ms and 450~800 ms; cluster-level corrected *p*s < 0.038). By contrast, connectivity from the ITG to IFG-tri decreased in the 5~10 Hz (approximately 0~250 ms) and in the 15~22 Hz (approximately 380~780 ms; cluster-level corrected *p*s < 0.012). In the iRiC condition, connectivity from the ITG

JNeurosci Accepted Manuscript

to the IFG-tri decreased in the 8~14 Hz range approximately from 400 to 650 ms (cluster-level corrected p = 0.004). By contrast, connectivity from the FG to the IFG-tri increased in the 14~22 Hz range between approximately 50~600 ms (cluster-level corrected p = 0.002). Additionally, connectivity from the PoCG to the IFG-tri decreased in the 7~11 Hz range during two clusters (approximately 50~250 ms and 550~800 ms; cluster-level corrected ps < 0.034).

Between-condition comparisons revealed a consistency effect, with stronger PoCG-to-IFG-tri connectivity for RiC than RC (16~25 Hz, approximately 0~750 ms; cluster-level corrected p = 0.002), but reduced ITG-to-IFG-tri connectivity (16~20 Hz, approximately 400~700 ms; cluster-level corrected p = 0.010). For the regularity effect, iRiC relative to RiC showed enhanced connectivity from the PoCG (22~30 Hz, approximately 300~580 ms; cluster-level corrected p = 0.040), ITG (15~21 Hz, approximately 50~800 ms; cluster-level corrected p = 0.002), and FG (14~21 Hz, approximately 50~700 ms; cluster-level corrected p = 0.002) to the IFG-tri. These findings suggest that sublexical processing involves directed interactions among posterior temporal and occipitotemporal regions and frontal regions, particularly the IFG-tri. Under conditions involving inconsistent phonological information (RiC and iRiC), connectivity patterns between these regions were differentially modulated.

DISCUSSION

Using high spatiotemporal-resolution SEEG, we try to distinguish neural activity potentially related to conflict detection versus inhibitory control during word reading. The regularity contrast varies the correspondence between a radical's and the whole character's pronunciation, whereas the consistency contrast varies the reliability of a radical in predicting pronunciations within a phonetic family. These contrasts capture demands associated with detecting phonological conflict, which we interpret as conflict detection. For inhibitory control, we focused on associations between neural oscillations and RT under the conflicting RiC and iRiC conditions, where the phonetic radical generates a competing pronunciation requiring suppression. We therefore reasoned that RT provides an index of the control

JNeurosci Accepted Manuscript

demands involved in resolving this competition, and that neural activity covarying with RT may provide evidence for the neural processes supporting inhibitory control.

Conflict detection-related effects were observed in the β band in the FG and in the θ and α band across the PoCG, PCun, ITG, MTG, and FG. Inhibitory control-related effects were initially observed in the IFG-tri, PrCG, ITG, and CS. After excluding non-specific RT-related effects through the control analyses and directly testing the interaction between neural oscillations and experimental condition, converging evidence identified α band activity in the IFG-tri and PrCG. Finally, GCA revealed directed interactions from posterior regions implicated in conflict detection to frontal regions implicated in inhibitory control. These interactions were modulated under conditions involving phonological conflict, with enhanced β band connectivity from the PoCG, ITG, and FG to the IFG-tri.

Sublexical processing refined by conflict detection and inhibitory control

Previous studies have manipulated the relationship between whole-character and radical-level information, such as phonetic regularity and consistency (Yum et al., 2014; C. Zhao et al., 2024; L. Zhou et al., 2013) or semantic transparency (Feldman & Siok, 1999; Yan et al., 2012; Yang et al., 2011). However, these investigations mainly adopted a linguistic or psycholinguistic perspective, focusing on condition-level contrasts (e.g., high vs. low regularity) to infer sublexical processing. The underlying logic is that, with lexical and perceptual properties well controlled, any observed behavioral or neural differences can be attributed to sublexical processing. Yet such condition-based contrasts may conflate multiple cognitive processes, limiting the resolution with which their distinct neural substrates. For instance, neural and behavioral responses to irregular characters may reflect not only sublexical activation but also the detection of conflicts between sublexical and lexical representations and the engagement of inhibitory control (Fedorenko, 2014; Fedorenko et al., 2012). Using trial-level LMM, our study distinguishes conflict detection from inhibitory control, revealing their distinct neural correlates and interplay. These findings support the view that word reading

JNeurosci Accepted Manuscript

is a multifaceted (Woolnough et al., 2022), interactive process (Liu et al., 2021), highlighting the critical role of resolving internal conflict and exerting cognitive control in word recognition (De Rom et al., 2023).

In the explanatory framework of the current research, the two cognitive processes can be integrated into an account of the temporal dynamics. Sublexical processing during oral word reading involves an initial detection of conflict between whole-character and sublexical phonological information, reflected in regularity- and consistency-related neural effects. This conflict signal is then communicated across relevant brain regions to engage inhibitory control mechanisms, suppressing task-irrelevant phonological information and ultimately supporting correct pronunciation. Consistent with this framework, overall, conflict detection-related effects occurred relatively early, inhibitory control-related effects occurred in a later time window, and directed functional connectivity was observed in the intervening period. Although some timings appear misaligned (e.g., the consistency- and regularity-related effect observed relatively late, whereas connectivity from the FG, ITG, and PoCG to the IFG-tri emerged earlier), this does not necessarily argue against our account. This is because the regions serving as sources and targets in the GCA are not exclusively dedicated to conflict detection or inhibitory control but participate in broader language processes (Fedorenko, 2014; Hickok & Poeppel, 2007; Price, 2012). Early directed connectivity may therefore reflect early information exchange rather than the onset of conflict detection or inhibition itself.

Inhibitory control: General vs. language-specific

To establish the role of specific brain regions in inhibitory control, we examined whether their neural activity predicted RT. In trials with conflicting sublexical cues (RiC, iRiC), RT variability reflects the efficiency of suppressing irrelevant phonological information. LMM analyses revealed that activity in the IFG-tri and PrCG predicted RTs in conflict, but not in non-conflict trials, indicating a specific role in interference resolution rather than general task preparation or motor execution. Notably, these effects were frequency-specific, primarily in the α bands,

JNeurosci Accepted Manuscript

which are associated with top-down inhibition (Cavanagh & Frank, 2014; Hwang et al., 2014; Pscherer et al., 2023; Schaum et al., 2021). These findings support inhibitory control during word reading, specifically to suppress misleading sublexical cues, and suggest that domain-general control mechanisms are selectively engaged in language processing when interference must be resolved (Fedorenko, 2014).

Although our task required a language-specific operation, the identified inhibitory control correlates were localized in the frontal cortex, a region implicated in domain-general suppression of irrelevant or conflicting information across diverse cognitive domains (Cavanagh & Frank, 2014; Fedorenko et al., 2013; Fu et al., 2022; Miller & Cohen, 2001). However, sublexical inhibition is not confined to frontal cortex: connectivity analyses revealed coordinated interactions between conflict-detection and inhibitory-control regions, highlighting that inhibitory control emerges from distributed network dynamics. These findings align with recent theoretical accounts (Wessel & Anderson, 2024), which propose that inhibitory control relies on a fronto-subthalamic mechanism, potentially reflected in β band activity across cortical networks.

Implications for recent theoretical frameworks of oral word reading

Our findings extend and refine recent theoretical accounts of oral word reading. The Dual Route Cascaded (DRC) model proposes that word pronunciation can be generated through both a lexical route and a sublexical route (Coltheart et al., 2001). In Chinese, whole-character and phonetic-radical phonology can converge or conflict, indexed by regularity and consistency, respectively. Previous studies have largely used these properties to characterize the influence of sublexical information on reading performance and neural activity (Yum et al., 2014; C. Zhao et al., 2024; L. Zhou et al., 2014). Our findings suggest that the consequences of such lexical–sublexical competition cannot be reduced to a unitary sublexical process. Rather, they involve at least two functionally distinguishable components: detecting the conflict between competing phonological representations and controlling the competing response. This

JNeurosci Accepted Manuscript

distinction provides a more specific account of what may occur when the outputs of lexical and sublexical processes do not converge. In particular, the present results suggest that posterior regions (including the PoCG, ITG, and FG) support conflict detection, whereas RT-associated activity in the frontal regions IFG-tri and PrCG is more closely related to the control required to resolve the resulting competition. Thus, whereas the DRC model captures the source of lexical–sublexical competition, our findings identify conflict detection and inhibitory control as explicit components of oral reading that resolve it, with neurocognitive evidence supporting this dissociation.

The conflict detection and inhibitory control processes can also be situated within a broader Binding and Retrieval in Action Control (BRAC) framework (Beste et al., 2023; Frings et al., 2020). From a Theory of Event Coding perspective (Hommel et al., 2001), when a Chinese character is initially learned, its orthographic, phonological, and semantic features can be integrated into an action-related representation. When the character is encountered again, both the sublexical and whole-character phonological representation can be retrieved. If these representations specify incompatible pronunciations (i.e., irregular or inconsistent characters), their co-activation may induce response conflict. Thus, conflict detection in our study can be understood as emerging from the retrieval of incompatible feature representations. Resolving this conflict requires cognitive control to suppress the competing sublexical response and select the appropriate pronunciation, while inhibitory control can be viewed as part of a broader process of updating and re-binding the appropriate response to the current stimulus.

The oscillatory findings are also compatible with this framework (Beste et al., 2023). The RT-controlled regularity effects were characterized by θ activity in the PoCG and α activity across the temporal cortex and PCun. These posterior effects may reflect the retrieval of lexical and sublexical phonological representations, consistent with previous evidence implicating θ and α dynamics in feature integration (Pastötter et al., 2024; Wendiggensen et al., 2022, 2023). In contrast, RT-associated effects were concentrated in α band activity in the IFG-tri and PrCG, potentially reflecting the control required to suppress competing pronunciations

JNeurosci Accepted Manuscript

and establish an appropriate stimulus–response mapping. This re-binding account is consistent with evidence linking α/β dynamics to perception–action integration and the maintenance of established representations (Geissler et al., 2024; Pastötter et al., 2025; Zhupa & Beste, 2026).

Behavioral-neural dissociation of the regularity effect

Although the neural analyses revealed significant regularity effects across several regions, the behavioral analysis showed no corresponding RT effect. This dissociation may reflect differences in information captured by behavioral and neural measures (Beste, 2021). RT is a composite measure integrating multiple processing stages, including perceptual analysis, evidence accumulation, response selection, and phonological articulation. Thus, regularity-related effects may be attenuated when aggregated into a single behavioral measure, whereas activity in specific regions and frequency may provide more sensitive indices of these processes. Second, although irregular characters impose greater processing demands and tend to slow reading, compensatory recruitment within the distributed reading network may offset the behavioral costs. Consistent with this possibility, a recent cTBS-fMRI study showed that perturbation of one language pathway can induce adaptive recruitment and enhanced connectivity in other components of the network, helping preserve behavioral performance (Luo et al., 2024). Similarly, our neural findings revealed bidirectional RiC–iRiC modulations, with greater θ activity in the PoCG but reduced α activity in the ITG, MTG, FG, and PCun for irregular-inconsistent characters. Thus, the neural RiC–iRiC contrast may capture regularity-related processing without necessarily producing a reliable overt RT cost at the group level.

Limitations

Several limitations of the present study warrant consideration. First, SEEG contacts was clinically determined, restricting recordings to specific cortical regions and potentially underestimating broader network involvement. Second, the study focused on monosyllabic single-character reading; future work should examine whether similar conflict and inhibition mechanisms operate in multi-

JNeurosci Accepted Manuscript

character words or sentence contexts. Third, while GCA indicates directional influence, it does establish definitive causality. Combining SEEG with perturbation techniques (e.g., transcranial magnetic stimulation or electrical stimulation), could help directly test the causal roles of the identified regions. Finally, because the pairwise GCA did not condition on the remaining regions in the network, the observed directional influences cannot exclude the possibility of common-driver or indirect effects from other regions.

Conclusion

This study reveals that word reading engages dissociable neural processes for sublexical conflict detection and inhibitory control, supported by low-frequency activity in posterior (FG, PoCG, PCun, ITG, and MTG) and frontal (IFG-tri and PrCG) regions, respectively. SEEG-based GCA further demonstrates directed posterior-to-frontal influence from detection to control regions, enabling the suppression of irrelevant cues for accurate recognition.

JNeurosci Accepted Manuscript

REFERENCES

Barnett, L., & Seth, A. K. (2014). The MVGC multivariate Granger causality toolbox: A new approach to Granger-causal inference. Journal of Neuroscience Methods, 223, 50–68. https://doi.org/10.1016/j.jneumeth.2013.10.018

Beste, C. (2021). Disconnected psychology and neuroscience—Implications for scientific progress, replicability and the role of publishing. Communications Biology, 4(1), 1099. https://doi.org/10.1038/s42003-021-02634-9

Beste, C., Münchau, A., & Frings, C. (2023). Towards a systematization of brain oscillatory activity in actions. Communications Biology, 6(1), 137. https://doi.org/10.1038/s42003-023-04531-9

Borghesani, V., Hinkley, L. B. N., Ranasinghe, K. G., Thompson, M. M. C., Shwe, W., Mizuiri, D., Lauricella, M., Europa, E., Honma, S., Miller, Z., Miller, B., Vossel, K., Henry, M. M. L., Houde, J. F., Gorno-Tempini, M. L., & Nagarajan, S. S. (2020). Taking the sublexical route: Brain dynamics of reading in the semantic variant of primary progressive aphasia. Brain, 143(8), 2545–2560. https://doi.org/10.1093/brain/awaa212

Borgwaldt, S. R., Hellwig, F. M., & Groot, A. M. B. D. (2005). Onset Entropy Matters – Letter-to-phoneme Mappings in Seven Languages. Reading and Writing, 18(3), 211–229. https://doi.org/10.1007/s11145-005-3001-9

Brainard, D. H. (1997). The Psychophysics Toolbox. Spatial Vision, 10(4), 433–436. https://doi.org/10.1163/156856897X00357

Cavanagh, J. F., & Frank, M. J. (2014). Frontal theta as a mechanism for cognitive control. Trends in Cognitive Sciences, 18(8), 414–421. https://doi.org/10.1016/j.tics.2014.04.012

Coltheart, M., Rastle, K., Perry, C., Langdon, R., & Ziegler, J. (2001). DRC: A dual route cascaded model of visual word recognition and reading aloud.

JNeurosci Accepted Manuscript

Psychological Review, 108(1), 204–256. https://doi.org/10.1037/0033-295X.108.1.204

Dang, M., Zhang, R., Wang, X., & Yang, J. (2019). The Interaction Between Phonological and Semantic Processing in Reading Chinese Characters. Frontiers in Psychology, 9, 2748. https://doi.org/10.3389/fpsyg.2018.02748

De Rom, M., Szmalec, A., & Van Reybroeck, M. (2023). The involvement of inhibition in word and sentence reading. Reading and Writing, 36(5), 1283–1318. https://doi.org/10.1007/s11145-022-10337-8

Delorme, A., & Makeig, S. (2004). EEGLAB: An open source toolbox for analysis of single-trial EEG dynamics including independent component analysis. Journal of Neuroscience Methods, 134(1), 9–21. https://doi.org/10.1016/j.jneumeth.2003.10.009

Fedorenko, E. (2014). The role of domain-general cognitive control in language comprehension. Frontiers in Psychology, 5. https://doi.org/10.3389/fpsyg.2014.00335

Fedorenko, E., Duncan, J., & Kanwisher, N. (2012). Language-Selective and Domain-General Regions Lie Side by Side within Broca's Area. Current Biology, 22(21), 2059–2062. https://doi.org/10.1016/j.cub.2012.09.011

Fedorenko, E., Duncan, J., & Kanwisher, N. (2013). Broad domain generality in focal regions of frontal and parietal cortex. Proceedings of the National Academy of Sciences, 110(41), 16616–16621. https://doi.org/10.1073/pnas.1315235110

Feldman, L. B., & Siok, W. W. T. (1999). Semantic Radicals Contribute to the Visual Identification of Chinese Characters. Journal of Memory and Language, 40(4), 559–576. https://doi.org/10.1006/jmla.1998.2629

Frings, C., Hommel, B., Koch, I., Rothermund, K., Dignath, D., Giesen, C., Kiesel, A., Kunde, W., Mayr, S., Moeller, B., Möller, M., Pfister, R., & Philipp, A.

JNeurosci Accepted Manuscript

(2020). Binding and Retrieval in Action Control (BRAC). Trends in Cognitive Sciences, 24(5), 375–387. https://doi.org/10.1016/j.tics.2020.02.004

Fu, Z., Beam, D., Chung, J. M., Reed, C. M., Mamelak, A. N., Adolphs, R., & Rutishauser, U. (2022). The geometry of domain-general performance monitoring in the human medial frontal cortex. Science, 376(6593), eabm9922. https://doi.org/10.1126/science.abm9922

Geissler, C. F., Schöpper, L.-M., Engesser, A. F., Beste, C., Münchau, A., & Frings, C. (2024). Turning the Light Switch on Binding: Prefrontal Activity for Binding and Retrieval in Action Control. Journal of Cognitive Neuroscience, 36(1), 95–106. https://doi.org/10.1162/jocn_a_02071

Geweke, J. (1982). Measurement of Linear Dependence and Feedback between Multiple Time Series. Journal of the American Statistical Association, 77(378), 304–313. https://doi.org/10.1080/01621459.1982.10477803

Granger, C. W. J. (1969). Investigating Causal Relations by Econometric Models and Cross-spectral Methods. Econometrica, 37(3), 424. https://doi.org/10.2307/1912791

Hickok, G., & Poeppel, D. (2007). The cortical organization of speech processing. Nature Reviews Neuroscience, 8(5), 393–402. https://doi.org/10.1038/nrn2113

Hommel, B., Müsseler, J., Aschersleben, G., & Prinz, W. (2001). The Theory of Event Coding (TEC): A framework for perception and action planning. Behavioral and Brain Sciences, 24(5), 849–878. https://doi.org/10.1017/S0140525X01000103

Hsu, C.-H., Lee, C.-Y., & Marantz, A. (2011). Effects of visual complexity and sublexical information in the occipitotemporal cortex in the reading of Chinese phonograms: A single-trial analysis with MEG. Brain and Language, 117(1), 1–11. https://doi.org/10.1016/j.bandl.2010.10.002

JNeurosci Accepted Manuscript

759 Hwang, K., Ghuman, A. S., Manoach, D. S., Jones, S. R., & Luna, B. (2014).
760 Cortical Neurodynamics of Inhibitory Control. The Journal of Neuroscience,
761 34(29), 9551–9561. https://doi.org/10.1523/JNEUROSCI.4889-13.2014

762 Kang, N., & Saito, S. (2025). Phonological processing of Japanese Kanji word by
763 L1-Chinese learners of Japanese: Verification of consistency and frequency
764 effects. Applied Psycholinguistics, 46, e16.
765 https://doi.org/10.1017/S0142716425000128

766 Lee, C.-Y. (2008). Rethinking of the regularity and consistency effects in reading.
767 Language and Linguistics, 9(1), 177–186.

768 Lee, C.-Y., Tsai, J.-L., Su, E. C.-I., Tzeng, O. J. L., & Hung, D. L. (2005).
769 Consistency, regularity, and frequency effects in naming Chinese characters.
770 Language and Linguistics, 6(1), 75–107.

771 Libben, G., Gibson, M., Yoon, Y. B., & Sandra, D. (2003). Compound fracture: The
772 role of semantic transparency and morphological headedness. Brain and
773 Language, 84(1), 50–64. https://doi.org/10.1016/S0093-934X(02)00520-5

774 Liu, Y., Shi, G., Li, M., Xing, H., Song, Y., Xiao, L., Guan, Y., & Han, Z. (2021).
775 Early Top-Down Modulation in Visual Word Form Processing: Evidence From
776 an Intracranial SEEG Study. The Journal of Neuroscience, 41(28), 6102–
777 6115. https://doi.org/10.1523/JNEUROSCI.2288-20.2021

778 Luo, Y., Wang, K., Jiao, S., Zeng, J., & Han, Z. (2024). Distinct parallel activation
779 and interaction between dorsal and ventral pathways during phonological and
780 semantic processing: A cTBS-fMRI study. Human Brain Mapping, 45(1),
781 e26569. https://doi.org/10.1002/hbm.26569

782 Maris, E., & Oostenveld, R. (2007). Nonparametric statistical testing of EEG- and
783 MEG-data. Journal of Neuroscience Methods, 164(1), 177–190.
784 https://doi.org/10.1016/j.jneumeth.2007.03.024

785 Martensen, H., Maris, E., & Dijkstra, T. (2000). When does inconsistency hurt? On
786 the relation between phonological consistency effects and the reliability of

JNeurosci Accepted Manuscript

sublexical units. Memory & Cognition, 28(4), 648–656. https://doi.org/10.3758/BF03201254

Miller, E. K., & Cohen, J. D. (2001). An Integrative Theory of Prefrontal Cortex Function. Annual Review of Neuroscience, 24(1), 167–202. https://doi.org/10.1146/annurev.neuro.24.1.167

Oostenveld, R., Fries, P., Maris, E., & Schoffelen, J.-M. (2011). FieldTrip: Open Source Software for Advanced Analysis of MEG, EEG, and Invasive Electrophysiological Data. Computational Intelligence and Neuroscience, 2011, 1–9. https://doi.org/10.1155/2011/156869

Pastötter, B., Beste, C., Münchau, A., & Frings, C. (2025). Perception–Action Integration Is Linked to Posterior Alpha/Beta Desynchronization. Journal of Cognitive Neuroscience, 37(11), 1913–1928. https://doi.org/10.1162/JOCN.a.52

Pastötter, B., Haciahmet, C. C., Beste, C., Münchau, A., & Frings, C. (2024). The interplay of cognitive control and feature integration: Insights from theta oscillatory dynamics during conflict processing. Cerebral Cortex, 34(8), bhae326. https://doi.org/10.1093/cercor/bhae326

Price, C. J. (2012). A review and synthesis of the first 20years of PET and fMRI studies of heard speech, spoken language and reading. NeuroImage, 62(2), 816–847. https://doi.org/10.1016/j.neuroimage.2012.04.062

Pscherer, C., Wendiggensen, P., Mückschel, M., Bluschke, A., & Beste, C. (2023). Alpha and theta band activity share information relevant to proactive and reactive control during conflict-modulated response inhibition. Human Brain Mapping, 44(17), 5936–5952. https://doi.org/10.1002/hbm.26486

Regev, T. I., Kim, H. S., Chen, X., Affourtit, J., Schipper, A. E., Bergen, L., Mahowald, K., & Fedorenko, E. (2024). High-level language brain regions process sublexical regularities. Cerebral Cortex, 34(3), bhae077. https://doi.org/10.1093/cercor/bhae077

JNeurosci Accepted Manuscript

Schaum, M., Pinzuti, E., Sebastian, A., Lieb, K., Fries, P., Mobascher, A., Jung, P., Wibral, M., & Tüscher, O. (2021). Right inferior frontal gyrus implements motor inhibitory control via beta-band oscillations in humans. eLife, 10, e61679. https://doi.org/10.7554/eLife.61679

Stokes, P. A., & Purdon, P. L. (2017). A study of problems encountered in Granger causality analysis from a neuroscience perspective. Proceedings of the National Academy of Sciences, 114(34). https://doi.org/10.1073/pnas.1704663114

Thiebaut De Schotten, M., & Forkel, S. J. (2022). The emergent properties of the connected brain. Science, 378(6619), 505–510. https://doi.org/10.1126/science.abq2591

Wendiggensen, P., Adelhöfer, N., Jamous, R., Mückschel, M., Takacs, A., Frings, C., Münchau, A., & Beste, C. (2022). Processing of embedded response plans is modulated by an interplay of frontoparietal theta and beta activity. Journal of Neurophysiology, 128(3), 543–555. https://doi.org/10.1152/jn.00537.2021

Wendiggensen, P., Prochnow, A., Pscherer, C., Münchau, A., Frings, C., & Beste, C. (2023). Interplay between alpha and theta band activity enables management of perception-action representations for goal-directed behavior. Communications Biology, 6(1), 494. https://doi.org/10.1038/s42003-023-04878-z

Wessel, J. R., & Anderson, M. C. (2024). Neural mechanisms of domain-general inhibitory control. Trends in Cognitive Sciences, 28(2), 124–143. https://doi.org/10.1016/j.tics.2023.09.008

Woolnough, O., Donos, C., Curtis, A., Rollo, P. S., Roccaforte, Z. J., Dehaene, S., Fischer-Baum, S., & Tandon, N. (2022). A Spatiotemporal Map of Reading Aloud. The Journal of Neuroscience, 42(27), 5438–5450. https://doi.org/10.1523/JNEUROSCI.2324-21.2022

JNeurosci Accepted Manuscript

Yan, M., Zhou, W., Shu, H., & Kliegl, R. (2012). Lexical and sublexical semantic preview benefits in Chinese reading. Journal of Experimental Psychology: Learning, Memory, and Cognition, 38(4), 1069–1075. https://doi.org/10.1037/a0026935

Yang, J., Wang, X., Shu, H., & Zevin, J. D. (2011). Brain networks associated with sublexical properties of Chinese characters. Brain and Language, 119(2), 68–79. https://doi.org/10.1016/j.bandl.2011.03.004

Yum, Y. N., & Law, S. (2019). Interactions of age of acquisition and lexical frequency effects with phonological regularity: An ERP study. Psychophysiology, 56(10), e13433. https://doi.org/10.1111/psyp.13433

Yum, Y. N., Law, S.-P., Su, I.-F., Lau, K.-Y. D., & Mo, K. N. (2014). An ERP study of effects of regularity and consistency in delayed naming and lexicality judgment in a logographic writing system. Frontiers in Psychology, 5. https://doi.org/10.3389/fpsyg.2014.00315

Zhao, C., Liu, Y., Zeng, J., Luo, X., Sun, W., Luan, G., Liu, Y., Zhang, Y., Shi, G., Guan, Y., & Han, Z. (2024). Spatiotemporal Neural Network for Sublexical Information Processing: An Intracranial SEEG Study. The Journal of Neuroscience, 44(45), e0717242024. https://doi.org/10.1523/JNEUROSCI.0717-24.2024

Zhao, J., Li, Q.-L., Wang, J.-J., Yang, Y., Deng, Y., & Bi, H.-Y. (2012). Neural basis of phonological processing in second language reading: An fMRI study of Chinese regularity effect. NeuroImage, 60(1), 419–425. https://doi.org/10.1016/j.neuroimage.2011.12.074

Zhou, L., Fong, M. C.-M., Minett, J. W., Peng, G., & Wang, W. S.-Y. (2014). Pre-lexical phonological processing in reading Chinese characters: An ERP study. Journal of Neurolinguistics, 30, 14–26. https://doi.org/10.1016/j.jneuroling.2014.03.002

JNeurosci Accepted Manuscript

Zhou, L., Peng, G., Zheng, H.-Y., Su, I.-F., & Wang, W. S.-Y. (2013). Sub-lexical phonological and semantic processing of semantic radicals: A primed naming study. Reading and Writing, 26(6), 967–989. https://doi.org/10.1007/s11145-012-9402-7

Zhou, L., & Perfetti, C. (2021). Consistency and regularity effects in character identification: A greater role for global than local mapping congruence. Brain and Language, 221, 104997. https://doi.org/10.1016/j.bandl.2021.104997

Zhou, X., & Marslen-Wilson, W. (1999). The nature of sublexical processing in reading Chinese characters. Journal of Experimental Psychology: Learning, Memory, and Cognition, 25(4), 819–837. https://doi.org/10.1037/0278-7393.25.4.819

Zhupa, M., & Beste, C. (2026). A division of labor in perception-action integration via hierarchical alpha-beta to beta-gamma coupling and local catecholaminergic control. Communications Biology, 9(1), 284. https://doi.org/10.1038/s42003-026-09564-4

JNeurosci Accepted Manuscript

FIGURE LEGENDS

Figure 1. Schematic illustration of sublexical effects, experimental procedure, and analytical framework. **(A)** Illustration of the two sublexical effects examined in the present study: consistency and regularity. Examples of Chinese characters are provided to demonstrate how phonetic radicals provide pronunciation cues and how conflicts arise between sublexical and whole-character information. **(B)** Experimental procedure, including stimulus presentation (top), simultaneous SEEG recordings (middle), and participants' vocal responses (bottom). Participants were instructed to read the stimuli aloud as quickly and accurately as possible. In the SEEG recordings, amplitude reflects electrophysiological signals recorded from intracranial contacts, whereas in the audio recordings, amplitude represents the sound waveform. **(C)** Overall neural activations represent the combined activity of conflict detection and inhibitory control. Analytical framework for dissociating conflict detection and inhibitory control during sublexical processing. First, regions associated with conflict detection were identified by comparing neural activity between conflict and non-conflict conditions while controlling for RT. Second, regions associated with inhibitory control were identified by examining the relationship between neural activity and RT under conflict conditions. Finally, Granger causality analysis was performed between these two sets of regions to investigate the directed interactions underlying the transformation from conflict detection to inhibitory control.

Figure 2. Contact distribution and general sublexical effects. **(A)** A total of 2524 contacts were recorded from the 39 participants. After preprocessing, 443 outliers (black dots; 261 with resistance > 15 kΩ, 182 with TFR > 3 *SD*s) were removed, leaving 2081 contacts (orange dots) for further analysis. **(B)** Activation in these 2081 contacts was assessed relative to the baseline (−800~0 ms) across trials. Red (373), blue (870), yellow (321), and gray (517) markers denote contacts with positive, negative, mixed, and no significant activation, respectively. **(C)** Among 1564 responsive contacts, colored dots (12) denote effective regions meeting the criteria (≥ 20 contacts from ≥ 10 participants); dot size indicates the number of

JNeurosci Accepted Manuscript

contacts. Black dots mark regions that inadequately meet the criteria. Numbers in parentheses show the number of participants (before the comma) and the number of contacts. **(D)** Whole-brain averaged general sublexical effects across 1564 responsive contacts for consistency (left; RC vs. RiC) and regularity (middle; RiC vs. iRiC) contrasts. These time-frequency representations provide a descriptive overview of condition-related oscillatory differences across responsive contacts. The colorbar indicates *t*-values from *t*-tests at each time-frequency point. The contour lines highlight significant time-frequency clusters. IFG-tri: inferior frontal gyrus, triangular part; INS: insula; PrCG: precentral gyrus; PoCG: postcentral gyrus; STG: superior temporal gyrus; MTG: middle temporal gyrus; ITG: inferior temporal gyrus; FG: fusiform gyrus; PCun: precuneus; AG: angular gyrus; CS: calcarine sulcus; MOG: middle occipital gyrus.

Figure 3. RT-controlled sublexical effects for consistency **(A)** and regularity **(B)**. Consistency involves one significant brain region, while regularity involves five. For each brain region, the results are presented in four parts: (1) the region and the distribution of contacts from the participants within it; (2) LMM results for neural oscillations in the θ (orange), α (green), and β (blue) bands, with the x-axis time-locked to stimulus onset, the y-axis representing the regression coefficients (*β* value), and the rectangular bars indicate significant time window after cluster-based permutation; violin plots illustrating neural oscillations within the LMM-significant cluster for a representative participant (3) and across all participants (4) separated by condition, with scatter points representing individual trials and *p*-values indicating significant difference between conditions. RC: regular consistent condition; RiC: regular inconsistent condition; iRiC: irregular inconsistent condition.

Figure 4. RT-associated sublexical effects in the RiC **(A)** and iRiC **(B)** conditions. There are three significant brain regions in the RiC condition and two in the iRiC condition. For each brain region, the results are also presented in four parts: the first two parts have the same meaning as in ***Figure 3***, while the last two parts show the correlation between neural oscillations within the LMM-significant cluster and RT (with both α and β bands in PrCG significant, shown here for α only) for a representative participant and across all participants. Scatter points represent

JNeurosci Accepted Manuscript

individual trials, with *p*-values indicating significant correlations. Brain regions enclosed by dashed boxes denote effects that remained after control analyses.

Figure 5. Granger causality results between sublexical processing regions. Four pathways showed significant directed connectivity: two in the RC condition (column 1; PoCG→IFG-tri and ITG→IFG-tri), two in the RiC condition (column 3; PoCG→IFG-tri and ITG→IFG-tri), and three in the iRiC condition (column 5; ITG→IFG-tri, FG→IFG-tri, and ITG→PrCG). Results enclosed by dashed boxes denote comparisons between conditions (column 2: RC vs. RiC, consistency; column 4: RiC vs. iRiC, regularity). In each sub-diagram, the x-axis is time locked to stimulus onset, the y-axis represents frequency, and the z-axis shows baseline-corrected GCV (or *t*-values in condition comparisons). Contour lines highlight significant time-frequency clusters. GCV: Granger causal value.

JNeurosci Accepted Manuscript

Table 1. Information on the effective brain regions for subsequent analysis.

Brain regions	Abbr.	Number of contacts	Number of participants	Mean MNI		
				X	Y	Z
Inferior Frontal Gyrus, triangular part	IFG-tri	43*	10†	−44	30	13
Insula	INS	51	15	−38	3	3
Precentral Gyrus	PrCG	34	11	−41	−5	44
Postcentral Gyrus	PoCG	31	13	−49	−17	36
Superior Temporal Gyrus	STG	52	12	−56	−30	12
Middle Temporal Gyrus	MTG	123	19	−57	−31	−7
Inferior Temporal Gyrus	ITG	58	16	−52	−36	−19
Fusiform Gyrus	FG	45	15	−32	−42	−17
Precuneus	PCun	28	11	−11	−56	37
Angular Gyrus	AG	32	11	−42	−61	34
Calcarine Sulcus	CS	49	12	−14	−67	12
Middle Occipital Gyrus	MOG	92	17	−35	−78	20

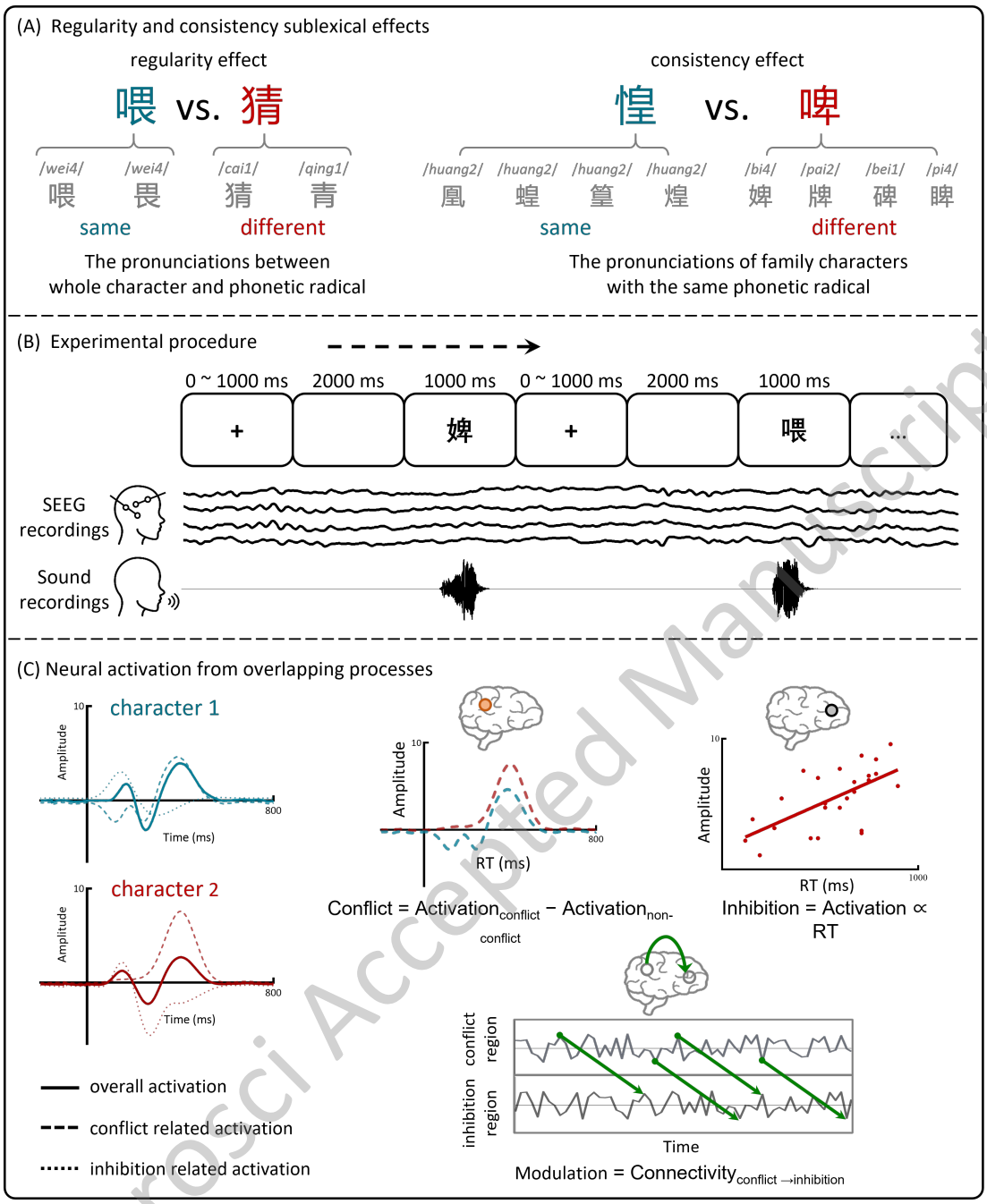
* The number of contacts contained within that brain region.

† How many participants these contacts come from.

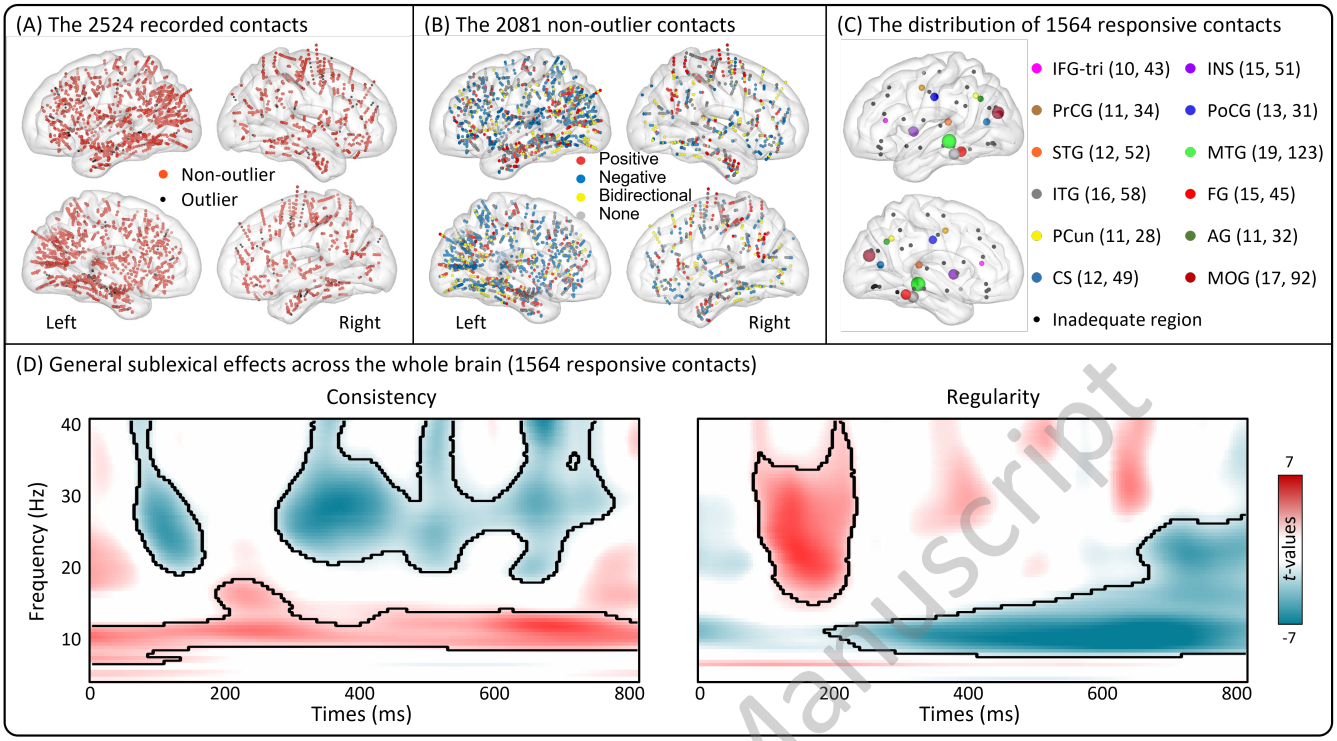
959

960

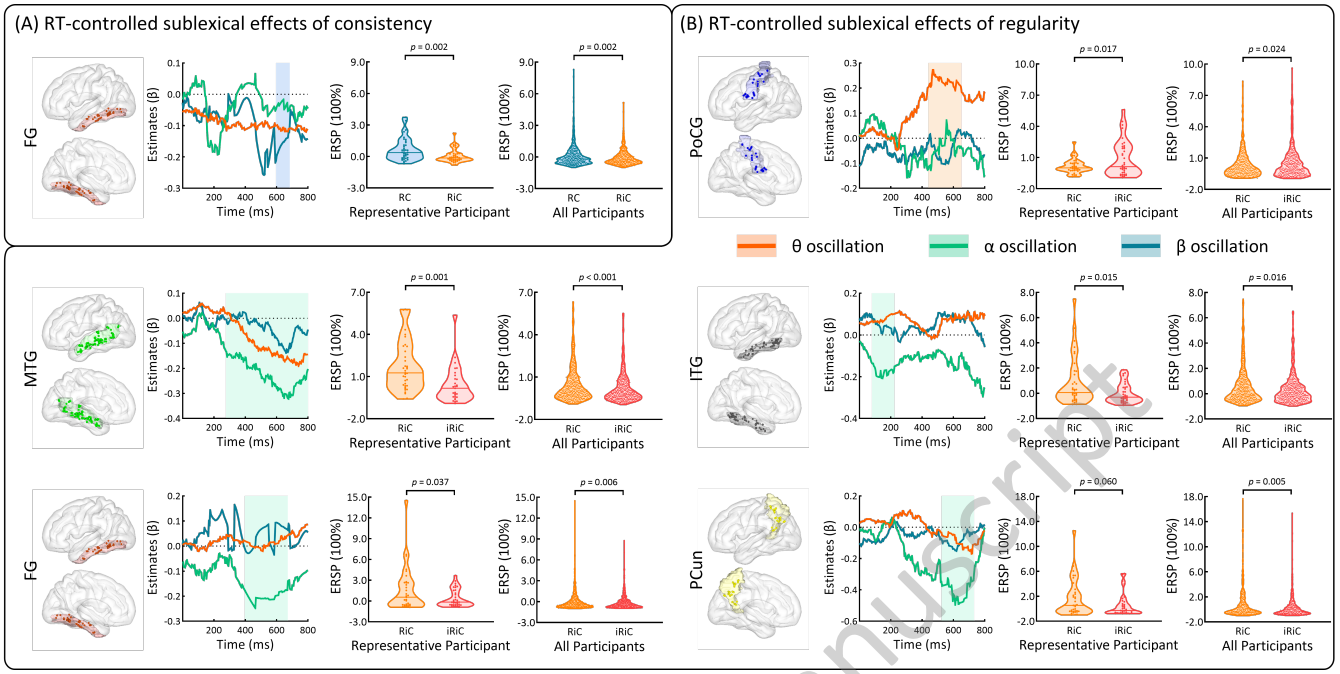
JNeurosci Accepted Manuscript



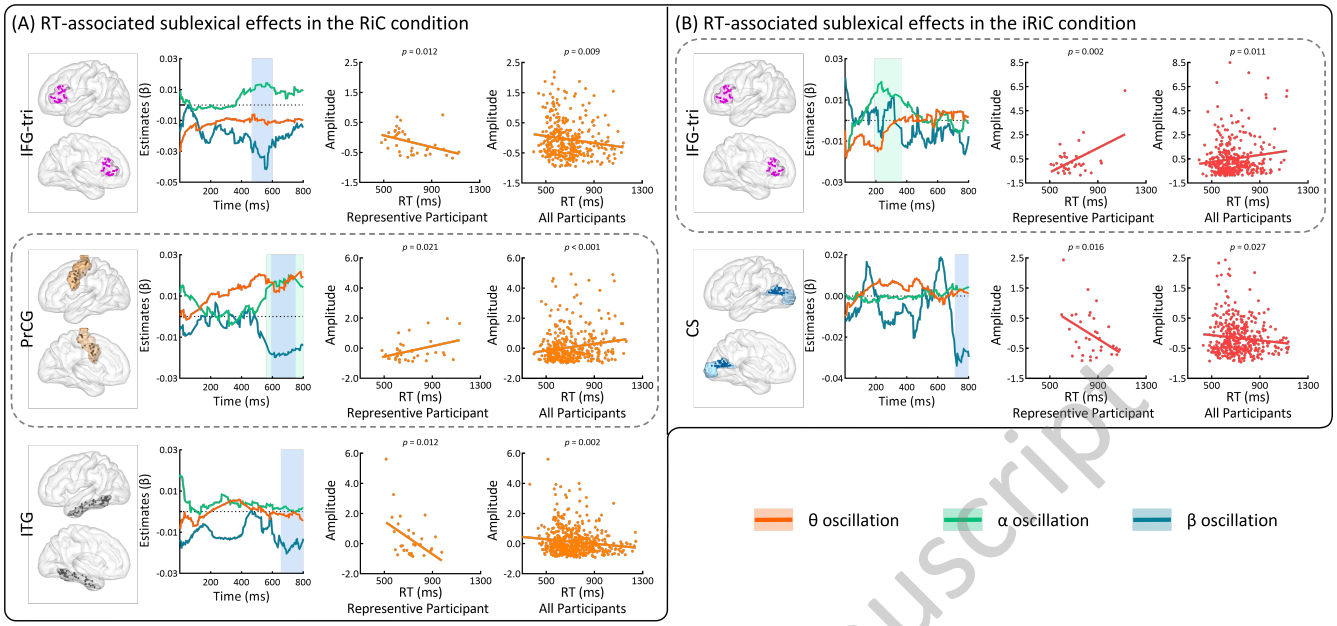
JNeurosci Accepted Manuscript



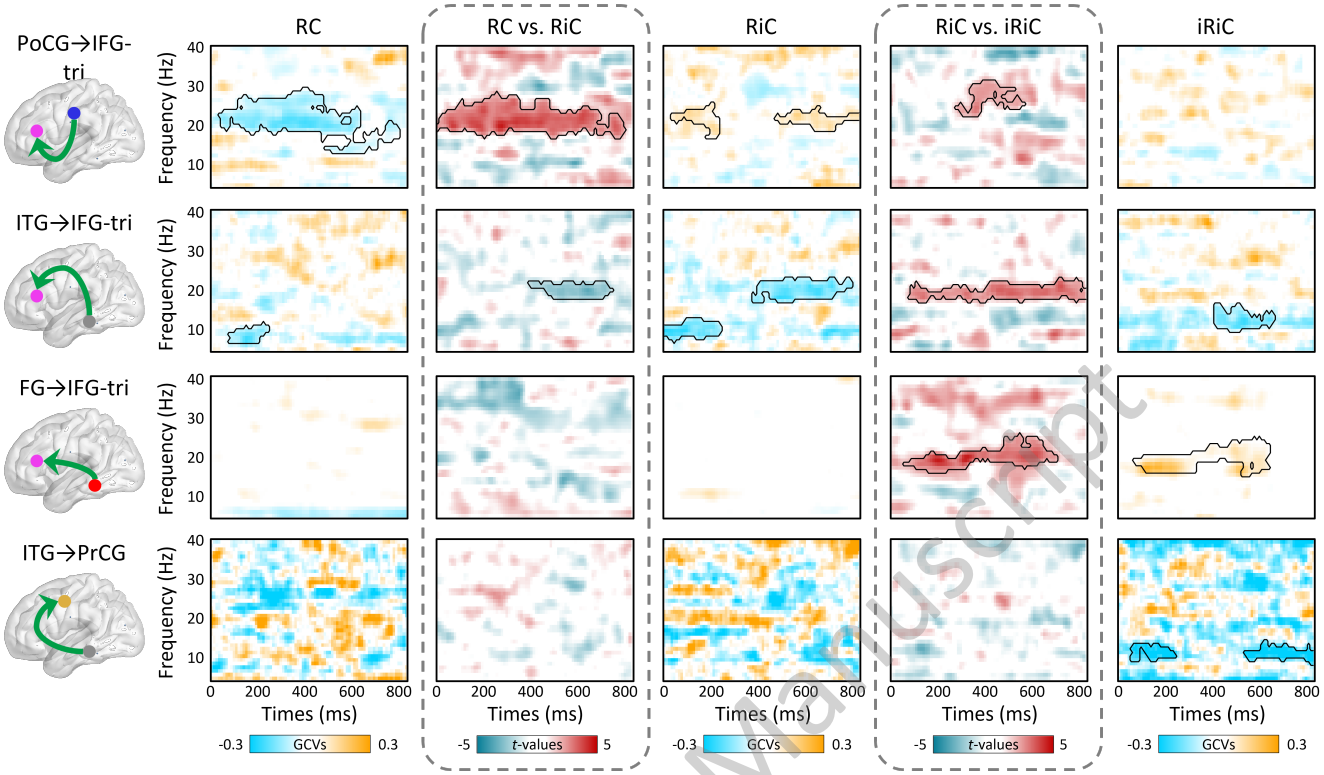
JNeurosci Accepted Manuscript



JNeurosci Accepted Manuscript



JNeurosci Accepted Manuscript



JNeurosci Accepted Manuscript